Lasers in Manufacturing Conference 2025

Laser-generated reflection gratings on shape memory actuators

Damian L. Haske[a,*], Jan Marx[a], Marvin Schuleit[a], Evgeny L. Gurevich[b], Cemal Esen[a], Andreas Ostendorf[a]

[a]*Applied Laser Technologies, Ruhr University Bochum, Universitätsstraße 150, 44801 Bochum, Germany*
[b]*Laser Center (LFM), University of Applied Sciences Münster, Stegerwaldstraße 39, 48565 Steinfurt, Germany*

Abstract

The employment of ultrashort laser pulses has enabled the fabrication of grating structures on a shape memory material, suitable for strain measurement by recording the interference pattern in the reflected light. This development signifies a novel application of laser-generated microstructures and facilitates direct strain measurement on the object without the necessity of an additional layer, as often required by conventional methods. The grating period was varied between 5 µm and 10 µm. Furthermore, Laser Induced Periodic Surface Structures (LIPSS) have been demonstrated to function as a grating structure for the purpose of producing lower grating periods. The application of LIPSS has been demonstrated to result in a grating period reduction down to approximately 620 nm. Moreover, the employment of LIPSS eliminates the requirement for monochromatic light in strain measurement applications. Illumination with a white light source leads to a color shift in the reflected light, which depends on the degree of stretching.

Keywords: LIPSS; NiTi; USP; tensile test; Bessel beam; shape memory effect

1. Introduction

Conventional strain measurement techniques generally necessitate physical contact with the workpiece or the utilization of specialized optical instruments. The objective of this study is to devise an optical technique that facilitates the measurement of the strain state of a shape memory actuator without the necessity of direct contact with the actuator during the measurement process. However, it should be noted that there exist optical measurement methods that necessitate the utilization of a sophisticated optical system. This paper presents two methods for optical strain measurement that enable strain to be measured on shape memory actuators using a simple setup.

The measurement of strain is of particular interest in shape memory alloys. Pseudoplastically deformed shape memory alloys (SMAs) demonstrate the capacity to revert to their original configuration during the phase transformation from strain-induced martensite to austenite. SMA actuators demonstrate the capacity to exert an exceptionally high actuating force in relation to their own mass. Furthermore, SMAs exhibit significant elastically deformable properties over an extensive range. According to the extant literature, elastic strains of up to 8 % have been documented in the context of SMA [Langbein et al., 2013].

According to the literature, SMA finds use in the manufacture of medical products, including stents for stabilizing arteries and wires for braces [Wichelhaus et al., 2005; Grossmann et al., 2022]. SMA actuators find application in industrial settings, such as the components of pneumatic valves [Schrittmatter et al., 2019]. These applications typically undergo thousands of expansion cycles. Consequently, frequent strain measurements are necessary to ascertain the fatigue behavior of the actuator.

* Corresponding author. Tel.: +49 234 32 15867
E-mail address: damian.haske@ruhr-uni-bochum.de

In this regard, the properties of shape memory alloys were being examined for their potential application in the fabrication of reflection gratings. It has been demonstrated that the LIPSS (Laser-Induced Periodic Surface Structures) on stainless steel exhibit a wavelength-dependent reflected light spectrum, indicating alterations in the material's elongation under illumination [Gräf et al., 2019]. The laser has been identified as a promising tool for the precise production of gratings, particularly in the context of SMAs, through the utilization of ultrashort pulses. The utilization of ultrashort pulses facilitates the structuring of materials with minimal thermal input. This fact is particularly salient given that the phase transformation temperature of shape memory alloys can be readily modified through the application of heat treatment [Carlucci et al., 2022]. This particular type of microstructuring and nanostructuring is especially well-suited for shape memory alloys, as the resulting structures exhibit minimal impact on the alloys' fatigue behavior [Marx et al., 2025].

2. Materials and Methods

The nickel-titanium alloy was selected as base material, which is distinguished by an austenite finish temperature of approximately 40 °C (NiTi - Nitinol Shape Memory Alloy Foil; 0.16 mm thick; A_f = 40 °C, Nexmetal Corporation, USA). This austenite finish temperature makes the material suitable for the use as actuator material. The samples for tensile testing were cutted by a ns-Laser to stripes with the dimensions of 2 mm × 27 mm × 0.16 mm.

The structures were produced using a femtosecond laser (Spectra-Physics Spitfire Ace, USA) with a central wavelength of 800 nm. The pulse duration was set to 110 fs and the repetition rate was set to 5 kHz for manufacturing. The structures were produced using a Bessel beam generated by an axicon with a 5° angle. The axicon focused the beam from a diameter of 8.3 mm (1/e²) to a spot diameter of 11 µm (1/e²). Compared to a Gaussian beam, a Bessel beam offers a greater depth of focus for machining. The Bessel beam is especially advantageous for complex geometries, such as those typically found in SMA components, as it eliminates the need for focus control [Marx et al., 2023].

During processing, the movement of the *x*-y-stage, to which the sample is attached, follows the path shown in Fig. 1. The laser was switched on during the movement of the stage to be able to neglect changes in speed that occur when the stage is accelerated. This technique is particularly well-known in the context of additive manufacturing, where it is referred to as 'skywriting'.

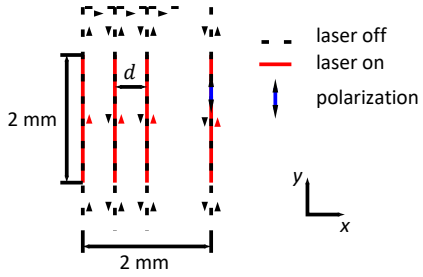

Fig. 1 Travel path of the axes during the production of the gratings

The laser-generated structures were characterized using a scanning electron microscope (EVO MA 10, Carl Zeiss Microscopy GmbH, Germany). Furthermore, the functional properties of the grating structures can be tested using the setup shown in Fig. 2. This setup consists of a fixture for the structured sample. A load can be applied to one side of the fixture. A triangulation sensor is installed on the same side to determine the real strain of the sample. A laser beam is directed onto the sample at an angle $\theta_i = 21.5°$. The interference pattern created by the grating can be captured with a moving camera mounted on an translational axis.

The position of the maxima of the intereference pattern of the reflected laser beam can be calculated using a geometric approach. At the distance $a = 90$ mm between the grating and the camera, perpendicular to the grating surface normal, the mth order maximum occurs at

$$M_m = a \cdot \tan\left(\arcsin\left(\frac{m \cdot \lambda}{d} + \sin(\theta_i)\right)\right), \tag{1}$$

with the grating period d, the wavelength of the incident laser beam λ and its incidence angle θ_i.

Greater elongation is accompanied by an increase in the distance between the structured lines, which is equivalent to an increase in the grating period. The detection of this change is facilitated by analyzing the interference pattern and measuring the distance between the maxima. As demonstrated in eq. (1), the distance between the maxima decreases as the grating period increases.

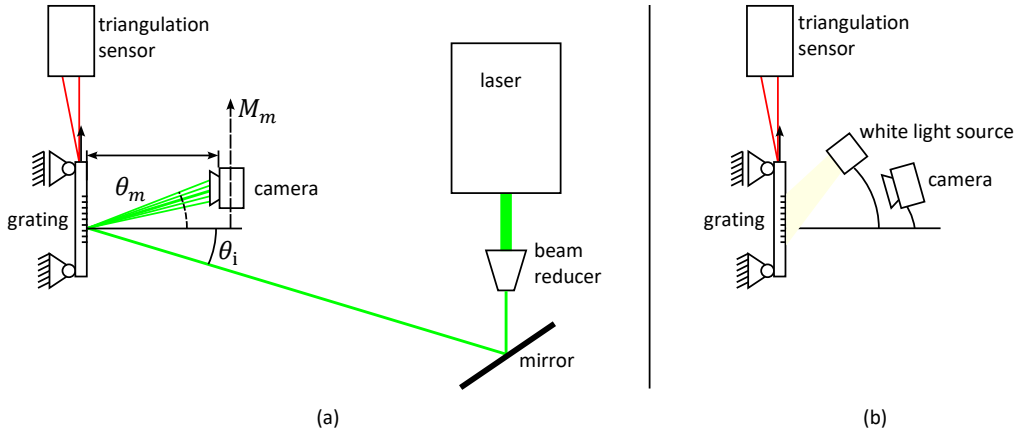

Fig. 2 Setups for optical strain detection. Gratings produced through direct laser writing can be analyzed using a laser source to assess strain based on the behavior of the interference pattern (a). The deformation of the grating during stretching, particularly for gratings fabricated LIPSS, can be detected by illuminating the grating with a white light source. The resulting visible color shift, caused by the alteration of the reflected wavelength, can be captured using a camera (b).

3. Results and Discussion

3.1 Manufacturing of gratings

The characteristics of the grating can be modified primarily by three parameters: fluence, pulse overlap, and, most significantly, the distance between the lines. The optimal conditions for achieving maximum effectivity included a fluence of 35 J/cm^2 and 53 J/cm^2, a pulse overlap between 95 and 99 %, and a line distance ranging from 5 to 10 µm. The gratings were examined using a scanning electron microscope. The results of this study are presented in Fig. 3. As the line distance increases, the areas where the surface remains unchanged increase concomitantly. In addition, a nanostructure with a period of approximately 620 nm was observed to be perpendicular to the structure resulting from the machining path. The line distance of 5 µm means that the entire surface was covered with LIPSS. It has been demonstrated that, due to the high regularity of the LIPSS, a second grid with a significantly smaller grating period than the line distance of the machining path was generated.

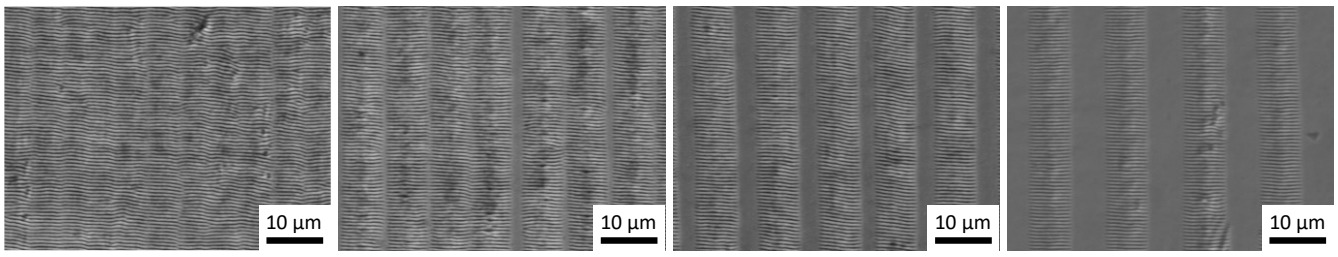

Fig. 3 SEM image of gratings manufactured with a fluence of 35 J/cm^2, 99 % pulse overlap and different line distance (a) 5 µm, (b) 7.5 µm, (c) 10 µm and (d) 12.5 µm.

3.2 Strain detection by analyzing interference patterns

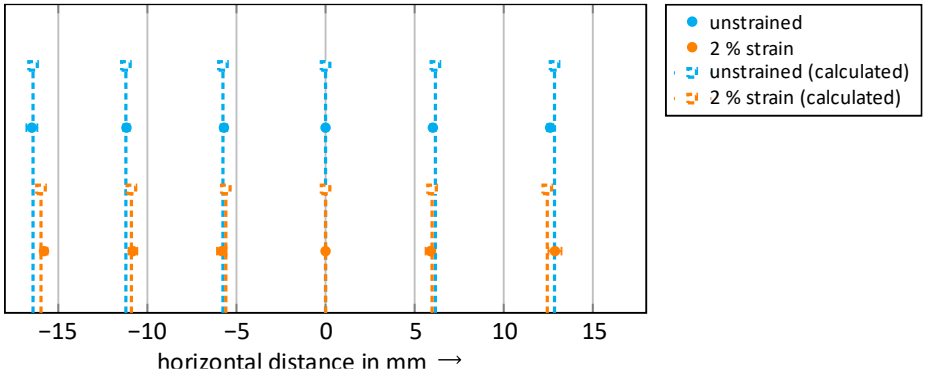

Fig. 4 Comparison between the real position of appearance of the maxima in the interferenze pattern and the calculated position. The grating was manufactured with a line distance of 10 µm, a fluence of 53 J/cm^2 and a pulse overlap of 95 % on a polished stripe of NiTi with an A_f = 45 °C.

Interference patterns were detected by illuminating the grating with a cw-laser with a wavelength of 532 nm (Verdi G, Coherent, Inc., USA). An industrial camera (UI-122xLE, IDS Imaging Development Systems GmbH, Germany), mounted on a linear stage, was used for detection. These camera images were stitched together to create a composite image from which intensity values were extracted. Intensity values were then be aggregated to generate intensity curves over horizontal distances. The position of the maxima was determined and compared to detect strain. Fig. 4 shows a good correlation between the actual and calculated maximum positions.

3.3 Strain detection by analyzing the change of the scattered wavelength

Another approach to strain detection involves using highly regular, self-organized nanostructures, such as high spatial frequency LIPSS, as gratings. The short grating period of 620 nm means that the first-order maxima occur at an angle of approximately 60°. This angle is high for period lengths in the range of several hundred nm, compared to gratings with a period of 10 µm, where the first-order maxima occur at an angle of approximately 3°. For this reason, the grating was illuminated with a white light source, and a digital single-lens mirrorless (DSLM) camera (OM-D E-M10 III, Olympus K.K., Japan) with a mounted macro lens (M.Zuiko Digital ED 60 mm F2.8 Macro, Olympus K.K., Japan) was used to observe the color change at an angle of 12°. The color change for different strain states is shown in Fig. 5. In this setup, the white light source is positioned at an angle of 47°. During stretching of the shape memory alloy, the camera and light source positions remained unchanged.

The grating equation demonstrates a proportional relationship between the reflected wavelength and the grating period. As shown in Fig. 5, a color change from blue (approximately 480 nm) to green (approximately 520 nm) indicates an elongation of approximately 8 %.

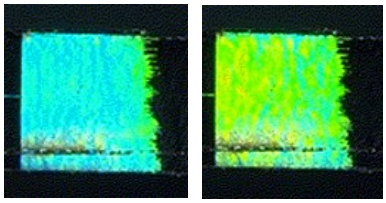

(a) (b)

Fig. 5 The reflected color depends on the applied strain. For instance, a color shift from blue in the unstrained state (a) to green in the strained state (b) is evident. This corresponds to a strain shift from 0 % to approximately 8 %.

4. Conclusion

The present study examined the fabrication of reflection gratings on shape memory actuators for strain measurement. Utilizing ultrashort laser pulses has enabled the fabrication of gratings with periods ranging from 5 to 12.5 µm, which are conducive to the generation of interference patterns. These grids were fabricated by means of direct laser writing on NiTi stripes. In addition to the aforementioned method of generating diffraction gratings, a grating period of approximately 620 nm was achieved by employing highly regular LIPSS. The strain measurement by analyzing the displacement of the diffraction orders was able to determine the strain near to the expected value. Furthermore, a color change in the light reflected on the grating has been observed when a white light source is directed onto the grating, indicating a distinction in strain states. These results are promising for contactless strain measurement on shape memory actuators.

References

Strittmatter, J., Gümpel, P., Hiefer, M., 2019, Intelligent materials in modern production – Current trends for thermal shape memory alloys, Procedia Manufacturing 30, p. 347–356.

Wichelhaus, A., Geserick, M., Hibst, R., Sander, F. G., 2005, The effect of surface treatment and clinical use on friction in NiTi orthodontic wires, Dental materials: official publication of the Academy of Dental Materials 21.10, p. 938–945.

Grossmann, S., Bohne, E., Senz, V., Grabow, N., Schmitz, K.-P., Siewert, S., 2022, Water-supported femtosecond laser ablation of Nitinol for cardiovascular stents, Current Directions in Biomedical Engineering 8.2, p. 455–458

Langbein, S., Czechowicz, A., 2013. Konstruktionspraxis Formgedächtnistechnik, Springer Fachmedien Wiesbaden, Wiesbaden

Marx, J., Schmelter, T., Schuleit, M., Haske, D., Stötzel, N., Frenzel, J., Eggeler, G., Kuhlenkötter, B., Esen, C., Ostendorf, A., 2025, Influence of Laser-Induced Surface Modifications on the Fatigue Behavior of SMA Wire Actuators, Shape Memory and Superelasticity

Gräf, S., Kunz, C., Undisz, A., Wonneberger, R., Rettenmayr, M., Müller, F. A., 2019, Mechano-responsive colour change of laser-induced periodic surface Structures, Applied Surface Science 471, p. 645–651.

Carlucci, G., Patriarca, L., Demir, A. G., Lemke, J. N., Coda, A., Previtali, B., Casati, R., 2022, Building Orientation and Heat Treatments Effect on the Pseudoelastic Properties of NiTi Produced by LPBF, Shap. Mem. Superelasticity 8, p. 235–247

Marx, J., Gurevich, E. L., Schuleit, M., Esen, C., Ostendorf, A., 2023, Bessel beam generated LIPSS on NiTi wires, Appl. Phys. A 129